

**IDENTIFICATION OF GENES REGULATING SMURF2-INDUCED  
SENESCENCE IN HUMAN FIBROBLASTS USING  
GENOME-WIDE GENE KNOCKDOWN SCREENING**

A Major Qualifying Project Report

Submitted to the Faculty of the

WORCESTER POLYTECHNIC INSTITUTE

in partial fulfillment of the requirements for the

Degree of Bachelor of Science

in

Biology and Biotechnology

by

---

Tyler Doughty

April 30, 2009

APPROVED:

---

Hong Zhang, Ph.D.  
Cell Biology  
Umass Medical Center  
Major Advisor

---

David Adams, Ph.D.  
Biology and Biotechnology  
WPI Project Advisor

## **ABSTRACT**

Smurf2 is an E3 ligase previously identified by our laboratory to be up-regulated by telomere shortening in senescent cells, and is sufficient to induce senescence in early passage human cells. Both the p53 and pRB senescence pathways are utilized by Smurf2 to induce senescence, but the precise mechanism of Smurf2-induced senescence remains unknown. The purpose of this project was to identify genes downstream of Smurf2 in the senescence pathways using a genome-wide short hairpin RNA (shRNA) screen in human fibroblasts. Using this strategy, I have identified 13 potential modulators of Smurf2-induced senescence, including AHCYL1 and CDC42BPA. Preliminary analysis indicates that AHCYL1 regulates senescence via the Smurf2-p53 pathway.

# TABLE OF CONTENTS

Signature Page .....	1
Abstract .....	2
Table of Contents .....	3
Acknowledgements .....	4
Background .....	5
Project Purpose .....	15
Methods .....	16
Results .....	24
Discussion .....	36
Bibliography .....	40

## **ACKNOWLEDGEMENTS**

I would like to thank Professor Hong Zhang for the opportunity to perform this project in his lab, and for his continual support throughout the experimental and writing processes. I would like to thank Hang Cui for her assistance in setting up this project and the guidance, support, and patience she exhibited in doing so. I would also like to thank Yahui Kong and Charusheila Ramkumar for showing me how to carry out laboratory techniques, and for rescuing me from a precarious situation or two. Finally, I would like to thank Dave Adams for his assistance in choosing the right lab to study in, MQP editing, and for years of professional career advice.

# BACKGROUND

## Replicative Senescence

The *in vitro* culture of normal human fibroblasts results in a finite number of cell divisions before cells reach replicative senescence, a permanent arrest of growth (Hayflick and Moorehead, 1961). This arrest occurs in the G1/G0 stage of cell division (Sherwood et al., 1988), and is characterized by a variety of changes, including alterations in gene expression (Campisi et al., 1996), positive staining for B-gal at pH 6 (Dimitri et al., 1995), and cells become larger, flattened, and granular (Goldstein, 1990).

## Telomerase, and Telomere Shortening

Replicative senescence has been shown to be activated by the shortening of telomeres (Harley, 1991), specialized structures found at the end of chromosomes that contain variable numbers of DNA repeats of TTAGGG in humans (Blackburn, 2001). Telomeres are shortened each cell division due to the inability of DNA polymerase to replicate the ends of linear chromosomes completely (Watson, 1972). This shortening is counteracted by the non-template activity of the enzyme telomerase which adds telomeric repeat sequences to the end of the chromosome (Shippen-Lentz and Blackburn, 1989). The incomplete fill-in by DNA polymerase leaves a 3' overhang with the telomeric repeat sequence (Blackburn, 2001).

Most somatic cells have no telomerase activity (Kim et al., 1994), this means that they do not replace the lost telomeric repeats after DNA replication, resulting in the shortening of telomeres during each replication cycle (Zhang, 2007). Supporting the

hypothesis that telomere shortening activates senescence, it has been shown that expression telomerase's catalytic subunit (TERT) in cells susceptible to replicative senescence can prevent telomere shortening and delay senescent arrest by >20 doublings (Bodnar et al., 1998), whereas inhibition of telomerase in immortal cells limits their reproductive lifespan (Zhang et al. 1999), and furthermore, the longer telomeres are when telomerase is inactivated in immortal cells the greater the number of cell doublings before the onset of replicative senescence (Blackburn, 2001).

The precise mechanism by which telomere shortening activates replicative senescence has yet to be elucidated. One hypothesized mechanism suggests that the senescence pathway is triggered by the decrease in the amount of telomeric repeats leading to a change in the structure of the telomeric cap, a protein/DNA structure thought to keep DNA safe from degradation, leading to uncapping (Blackburn, 2001). This uncapping occurs naturally when telomeres shorten to critical lengths, and in the presence of telomerase, this uncapping allows telomeric repeats to be added (Blackburn, 2001). However, if telomerase is absent, telomeric caps remain open, potentially contributing to the aging phenotype via a yet unidentified mechanism (Blackburn, 2001).

### **Multiple Pathways Lead to Senescence**

An early set of experiments showed that certain immortal human cell lines can be induced into replicative senescence by cellular fusion with certain other immortal human cell lines (Pereira-Smith and Smith, 1988). The experiment showed that multiple groups of complementary immortal cell lines exist, and when members of different groups are fused, they no longer show immortal cell division. This result suggests that immortality in oncogenic cell lines is caused by the mutation of different senescence pathways, which

can be corrected by the introduction of an intact version of that pathway (even from another immortal line). In short, this data suggests that senescence is dominant, and that multiple pathways can cause senescence (Pereira-Smith and Smith, 1988).

### *p53 Senescence Pathway*

ATM (ataxia-telangiectasia mutated) and ATR (Rad3-related) kinases are members of the PI3K DNA damage response pathway, and have been shown to be up-regulated during senescence (Herbig et al., 2004). ATM is activated in response to dsDNA breaks, while ATR is activated by the presence of G-rich ssDNA, both of which may be present as the telomeres shorten (Herbig et al., 2004). These kinases are both capable of phosphorylating p53, which has been shown to trigger replicative senescence (Herbig et al., 2004, see Figure-1).

p53 triggers replicative senescence by binding DNA specifically and activating the transcription of growth inhibitory factors. Over-expression of p53 inhibits cell proliferation (Chen et al., 1990), while inhibition of p53 extends the proliferative lifespan in fibroblasts (Atadja et al., 1995). This inhibition of replicative potential is due to the activation of p53 which occurs in late passage cells during replicative senescence in response to telomere shortening (Goberdhan, 2005). This activation is the result of phosphorylation of p53 by ATM and/or ATR, which has been shown to raise p53's DNA binding activity; therefore up-regulating the transcription of growth regulating factors (Atadja et al., 1995). One of the major factors transcriptionally activated by p53 is p21, which has been linked with inhibition of normal cell growth in fibroblasts (Atadja et al., 1995). Human fibroblasts with p21 null mutations are able to escape senescence (Brown

et al. 1997), while expression of p21 has been shown to be sufficient in some cells to induce senescence (Goberdhan, 2005).

### *pRB Senescence Pathway*

Loss of Retinoblastoma, or pRB, expression has been shown to allow human fibroblasts to escape senescence (Wei et al., 2003). This senescent escape is thought to be the result of a pathway that acts alongside the p53 senescence pathway to keep senescent cells in growth arrest (Goberdhan, 2005). Retinoblastoma is found in a hypophosphorylated state in senescent cells (Goberdhan, 2005), this state increases pRB's ability to act as a transcriptional repressor; by allowing it to bind to and inactivate transcription factors (Ezhevsky et al., 1997). One notable transcription factor that pRB binds to and represses when hypophosphorylated is E2F, an important factor in DNA synthesis (Ezhevsky et al., 1997).

The hypophosphorylation of pRB is thought to be initiated/maintained by p16 and p21 (Stein et al. 1999; Goberdhan, 2005), both of which inhibit cyclin dependent kinases (CDKs), and are up regulated during senescence in human fibroblasts (Itahana et al., 2003). p21 may lead to the hypophosphorylated phenotype by interfering with the CDK2/Cyclin E kinases (Goberdhan, 2005). This link between p21 and pRB suggests that p53 can play a role in pRB senescence, by turning on p21, which inhibits pRB's kinases (see Figure-1). However, pRB can also be activated by p16 independently of the p53 pathway. p16 and its upstream activators have been shown to induce senescence in a pRB dependent, but p53 independent manner (Itahana et al., 2003). This suggests that pRB can be activated by p53 and can cause senescence on its own.



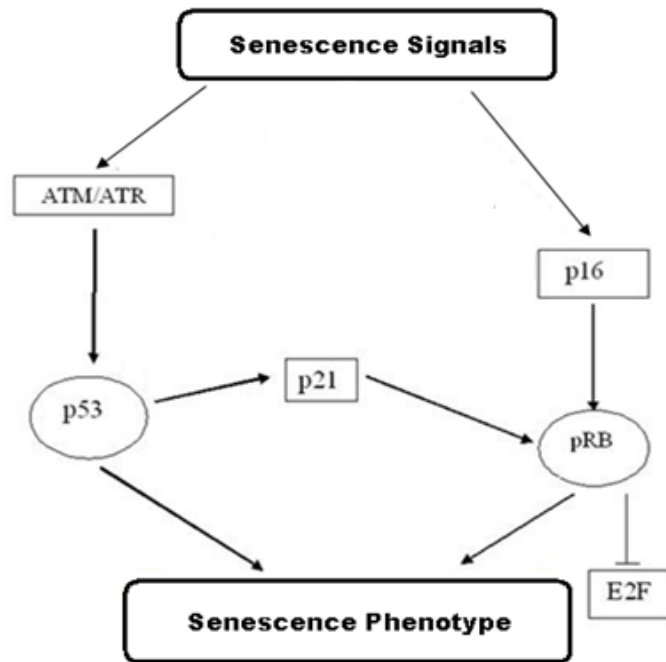


**Figure 1: An Overview of the p53 and pRB Senescence Pathways.** Shown are simplified signaling pathways that lead from senescence signals (stress, telomere shortening, DNA damage) to the senescence phenotype. Note that p53 and E2F (repressed by pRB) are transcription factors, and that upregulation of p53 and/or inhibition of E2F can cause changes in the expression of many genes, leading to the senescence phenotype.

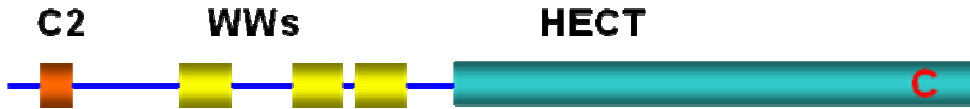
## Smurf2 and Senescence

Figure-1 above does not show the entire picture, due to the lack of complete understanding of all the factors involved and their connections to one another. The least established portions of this pathway are the key genes regulated by p53 expression and E2F inhibition, and the genes that act upstream of ATM/ATR and p16. One of the genes upstream of p16 and ATM/ATR is Smurf2, a protein of interest in our laboratory.

### *Smurf2 Protein Description*

Smurf2, or SMAD Specific E3 Ubiquitin Protein Ligase 2, is a human gene encoding a 748 amino acid protein involved in the ubiquitination of SMAD2, which leads

to proteosomal degradation of SMAD2, a key regulator of TGF- $\beta$  signaling (Lin et al., 2000).



**Figure 2: Diagram of the Smurf2 Protein.** The Smurf2 protein has three WW domains (yellow) which bind proline rich regions of other proteins. Smurf2 also contains C2 and HECT domains (Chen and Sudol, 1995). A cysteine (C) at position 716 of the protein is required for Smurf2's ubiquitin ligase function.

### *Smurf2 and Senescence*

Microarray analysis in our laboratory indicated that Smurf2 levels increase in response to telomere reduction, indicating that this protein may be involved in replicative senescence (Zhang and Cohen, 2004). Further study showed that early passage fibroblasts, including WS1 cells used in this MQP, that were induced to express Smurf2 at the levels similar to senescent cells showed premature replicative senescence (Zhang and Cohen, 2004). Moreover, the same cell lines first made immortal by hTERT expression were induced to senesce in the presence of Smurf2 (Zhang and Cohen, 2004).

Even Smurf2 mutants that are unable to perform ubiquitin ligase activity (specifically a substitution C716A that disrupts the catalytic pocket) are able to induce replicative senescence in fibroblasts, regardless of hTERT presence (Zhang and Cohen, 2004). This up-regulation of Smurf2, or Smurf2 C716A, sufficient for induction of senescence, did not correlate with significant changes in Smad2 or TGF- $\beta$  levels in the cell lines, suggesting that the Smurf2's ligase activity is not required for senescence (Zhang and Cohen, 2004).

### *Smurf2 and p53/pRB*

Smurf2 has been shown to induce senescence in the absence of an intact p53 pathway or pRB pathway (Zhang and Cohen, 2004). However, if both pathways are knocked out, Smurf2 expression does not lead to senescence, thus indicating that Smurf2 affects both the p53 and the pRB senescence pathways (Zhang and Cohen, 2004).

Two processes have been identified by which Smurf2 can influence pRB senescence (Figure-3). First Smurf2 acts to up-regulate p16 by degrading ID1/ID3 via its ubiquitin ligase function (Kong et al., unpublished). This degradation of ID1/ID3 increases p16 levels because ID1/ID3 functions to repress p16 transcription (Hara, 1996). Second Smurf2 increases p21 levels which blocks E2F via pRB (Cui et al., unpublished). Data suggests that Smurf2 increases p21 by signaling through a Notch3 intermediate (Cui et al., unpublished). The process by which Smurf2 influences p53 senescence has yet to be elucidated. The focus of this MQP project is to identify other effectors turned on by Smurf2 which play a role in this pathway.

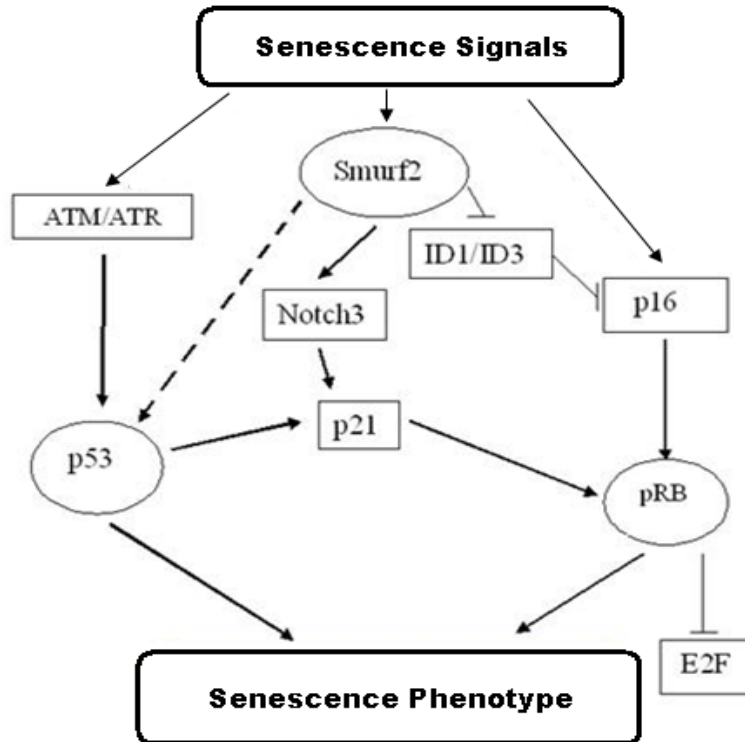
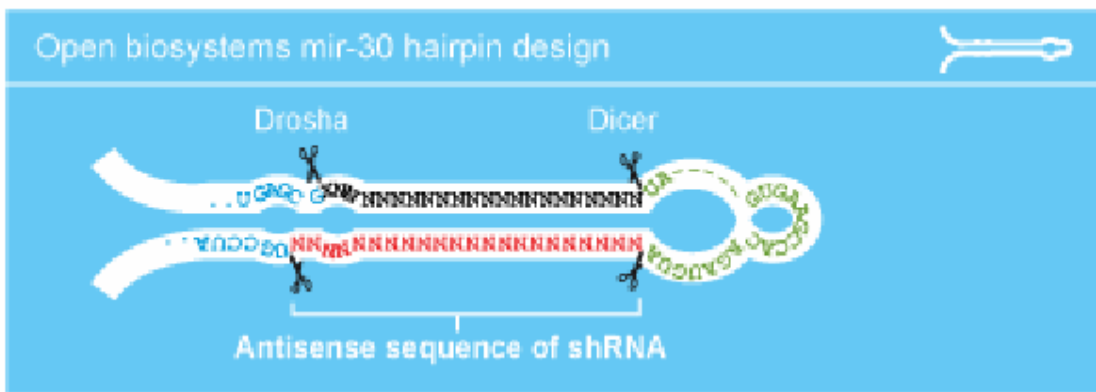


**Figure 3: Smurf2's Relation to p53 and pRB Senescence.** Smurf2 is up regulated in response to senescence signals, and its up-regulation has been shown to be sufficient to cause senescence in early passage fibroblasts. Smurf2 has been shown to up-regulate p16 mRNA and p21 levels, via suppression of ID1/ID3 and up-regulation of Notch3, respectively. Smurf2 has been shown to cause senescence in a pRB independent manner, and cannot cause senescence independently of pRB and p53; suggesting a link (dotted arrow) between Smurf2, p53, and senescence.

### Identification of Genes Downstream of Smurf2 Using shRNA Screening

This MQP study focused on the identification of signaling factors downstream of Smurf2, which play a key role in the cellular senescence pathway. I hypothesize that deficiency of an important signaling gene downstream of Smurf2 in the senescence pathway would interfere with the Smurf2-induced signal and consequently would allow primary fibroblasts to escape Smurf2-induced senescence. To test this hypothesis and identify genes downstream of Smurf2 in the senescence pathway, I used short hairpin RNA (shRNA) to systematically knockdown genes and identify candidate genes whose knockdown affects Smurf2-induced senescence.

The shRNA library was tested using commercially-obtained pools containing shRNA constructs inserted into plasmids capable of being packaged into lenti-virus. Pools used were from the Expression Arrest GIPZ Lentiviral shRNAmir Library from Open Biosystems. These shRNA constructs contained a hairpin sequence; comprised of two 22bp long sequences that would basepair to one another when translated to mRNA (see Figure-4).

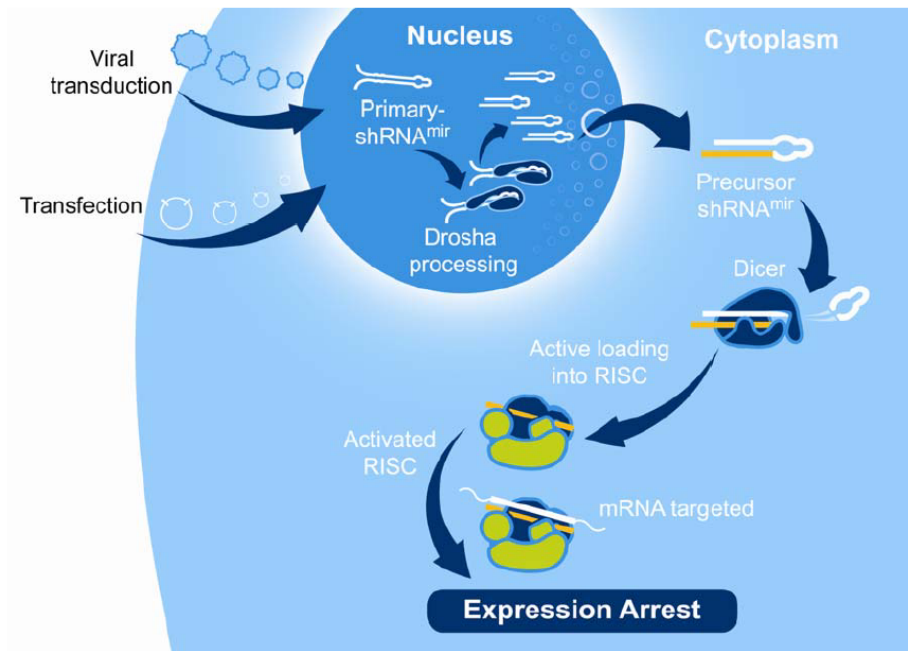


\*Figure from Open Biosystems, Expression Arrest GIPZ lentiviral shRNAmir library product information.

**Figure 4: Design of the shRNAmir Hairpins.** The shRNAmir system incorporates two 22 base pair sequences capable of binding each other on a transcribed mRNA. The dsRNA causes a cellular drosha/dicer response leading to RNA interference of transcript with an identical 22bp sequence.

When expressed, these shRNA constructs form a hairpin, which are cut by dicer/drosha resulting in two small interfering RNA, or siRNA, one that targets a known gene and one that is its antisense and has no function (see Figure-5). The sense siRNA binds to the complementary mRNA transcript sequence and destroys that transcript via the same dicer/drosha mechanism, resulting in expression arrest of that transcript (see Figure-5). The total number of unique shRNA constructs in the pools tested in this project was 30,000. This large number of unique shRNA constructs was utilized to identify potential genes that allow an escape of senescence. Cells were infected at an

MOI of 0.1 (a titer of virus predicted to infect individual cells with a single shRNA construct), and selected using puromycin (shRNA expressing virus encodes resistance to puromycin). The cells that received viral constructs survive, and are presumed to be producing a single 22bp siRNA capable of interfering with a single mRNA. This infection was then followed by infection with Smurf2-expressing viruses shown to cause cellular senescence in fibroblasts and another round of selection. This second selection incorporated puromycin to ensure the cells are expressing the shRNA encoding virus, and hygromycin (encoded by Smurf2 expressing virus) to ensure the cells are expressing the Smurf2 encoding virus.



\*Figure from Open Biosystems, Expression Arrest GIPZ lentiviral shRNAmir library product information.

**Figure 5: shRNAmir Expression Arrest Mechanism.** Cells that are transduced with a single virus containing a single shRNAmir construct can lead to expression arrest of a single transcript.

## **PROJECT PURPOSE**

Previous experiments in our laboratory indicated that over-expression of Smurf2 protein in early passage fibroblasts induces senescence (Zhang and Cohen, 2004). Smurf2 has been shown to induce senescence in the absence of an intact p53 pathway or pRB pathway, but if both pathways are knocked out Smurf2 expression does not lead to senescence. Thus, Smurf2 may affect both the p53 and the pRB senescence pathways (Zhang and Cohen, 2004). However, the complete set of genes involved in senescence and their interactions with one another have yet to be elucidated.

The purpose of this project was to identify potential genes in the senescence pathway that lie downstream of Smurf2 in order to facilitate a better understanding of senescence. Pools of shRNA encoding plasmids (30,000 unique shRNAs were tested in this project) were packaged into lentiviruses, and used to infect primary fibroblasts at a multiplicity of infection (MOI) of 0.1; to infect an average of one in 10 cells to ensure a single viral integration per infected cell. Cells were then infected with Smurf2 expressing virus to induce senescence. I hypothesized that cells that continued to grow after challenge with Smurf2 might contain an shRNA construct that interfered with the expression of a gene involved downstream of Smurf2 in the senescence pathway; and that knockdown of this gene disrupted the senescence signal elicited by Smurf2, thus allowing continued growth. Cells that escaped senescence grew into colonies, from which genomic DNA was extracted. PCR was run to amplify the shRNA construct contained by the cells of the colony. Sequencing later identified the siRNA sequence encoded by the senescence escaping cells, which was used to identify the gene knocked down in the escaping cells.

# METHODS

## **DNA Cloning**

DNA cloning was utilized in this project to amplify plasmid constructs used for viral packaging. These plasmids included pMD2-VSVG, pCMVdR8.74, and dsRed.

## *Cell Transformation*

Cell transformation was performed in XL-2 *E. coli* cell suspensions. Plasmid DNA was typically added at a concentration of 5 µg per sample. Samples were kept on ice for 30 minutes, heat shocked at 42°C for 30 seconds, then cooled on ice for 2 minutes. Cells were then cultured under ampicillin selection. When confluent, cultures were spun down at 4000 RPM, and plated on ampicillin plates. The next day single colonies were picked and amplified. Plasmids from these samples were collected via miniprep.

## *Plasmid Isolation*

Plasmid DNAs in this project were isolated using Quiagen's QIAprep® Spin Miniprep Kit.

## **DNA Transfection and Colony Forming Unit Determination**

This project required the stable expression of plasmid constructs in primary cells. In order to achieve this, DNA was delivered by lenti-viral constructs which integrate their contents into the genome of the infected host cell resulting in stable expression. Viruses packaged in this project included thirteen pGIPZ pools of shRNA plasmid constructs, Smurf2, and Smurf2 C716A (ligase mutant) plasmid constructs, and AHCYL1 and



CDC42BPA shRNA constructs. Colony forming units of each virus were quantitated to infect the primary cells in the screen at the proper multiplicity of infection.

#### *DNA Transfection in 293T*

Human embryonic kidney 293T (HEK-293T) cells were plated in DMEM medium with 10% fetal bovine serum, 100 U/mL penicillin, and 100 µg/mL streptomycin. These cells were cultured in a 37°C incubator at 5% CO<sub>2</sub> on 15cm tissue culture dishes. When their density was approximately 80% confluent, cells were freshly plated at a density of  $3.6 \times 10^6$  cells/ml on 10cm tissue culture dishes. Once the plates achieved ~70% density, they were transfected.

Transfection was performed in the 10cm plates using CaCl<sub>2</sub>/HBS transfection. The DNA to be packaged was mixed in a 15mL falcon tube with 6.5 µg of lenti-viral packaging vector pMD2-VSVG, 3.5 µg of lenti-viral envelope vector pCMVdR8.74, and 0.2 µg of dsRed (marker). The total volume of this mixture was raised to 437.5 µl using 0.1% TE. CaCl<sub>2</sub> was then added drop wise to the tube while vortexing at speed 7. Next, 500 µl of 2X HBS was added to the mixture drop wise. The final solution was added drop wise onto the HEK-293T cells in 10 ml of media. Twenty hours later the cells were observed under fluorescence microscopy for the presence of dsRed; plates with >50% of cells expressing dsRed were aspirated and fed with fresh media. Supernatants containing lentivirus were collected 24 hours later, and stored at -80°C to eliminate any living cellular contaminants.

#### *Colony Forming Unit Determination*

Colony forming units (CFUs) were determined for each virus made in this project. CFUs were determined in HT1080 cells plated at  $5 \times 10^4$  cells per 60cm plate. Each virus was used to infect four plates; three plates received a serial diluted volume of viral supernatant (10  $\mu$ l, 1  $\mu$ l, or 0.1  $\mu$ l), and one plate was used for a mock infection. All infections were performed in DMEM medium with 10% FBS, 100 U/mL penicillin, 100  $\mu$ g/mL streptomycin, and 4  $\mu$ g/mL polybrene. Twenty-four hours post infection, cells were aspirated and cultured in base media for 24 hours. After 24 hours, cells were plated in base media containing 1  $\mu$ g/mL puromycin or 300  $\mu$ g/mL hygromycin (depending on the resistance encoded on the plasmid).

Seven to ten days post infection, all plates were stained with 1% Crystal Violet in 3% ethanol for 5 minutes. Colonies on each plate were counted in order to determine the colony forming units per micro liter of viral supernatant.

### **shRNA Screening**

Gene knockdown screening using shRNA constructs allowed for the identification of genes involved in Smurf2-induced senescence. Two shRNA screens were run in this project; MOI 0.1 shRNA library with a Smurf2 challenge and MOI 0.1 shRNA library with a C716A challenge.

### *Cell Infection with shRNA Encoding Virus*

WS1 human embryo fibroblasts were plated at  $5 \times 10^5$  cells per 100cm plate. Each 100cm plate was infected with a single shRNA pool's viral supernatant at MOI 0.1 in media containing 4  $\mu$ g/mL polybrene. Two 60cm plates were plated at  $5 \times 10^4$  and were

mock infected (exposed to media containing 4  $\mu\text{g}/\text{mL}$  polybrene without receiving viral supernatant).

#### *Puromycin Selection*

The shRNA plasmid packaged into virus in this project encoded puromycin resistance. Two days post infection cells were challenged with media containing 1  $\mu\text{g}/\text{mL}$  puromycin. The mock infected plate was clear after about 72 hours of puromycin exposure. At this time the infection below was performed.

#### *Cell Infection with Smurf2/C716A Encoding Virus*

WS1 cells that survived puromycin exposure were then infected with Smurf2 viral supernatant that corresponded to  $2 \times 10^5$  Smurf2 virions per 100cm plate. This infection was performed in media containing 4  $\mu\text{g}/\text{mL}$  polybrene, alongside a mock infected 60cm plate.

#### *Puromycin/Hygromycin Selection*

The Smurf2, and Smurf2 C716A viruses used in this project encoded hygromycin resistance. Two days post infection with Smurf2/C716A, cells were challenged with media containing 0.5  $\mu\text{g}/\text{mL}$  puromycin and 150  $\mu\text{g}/\text{mL}$  hygromycin. Cells were maintained in this media for twenty days until colonies formed in the 100cm plates.

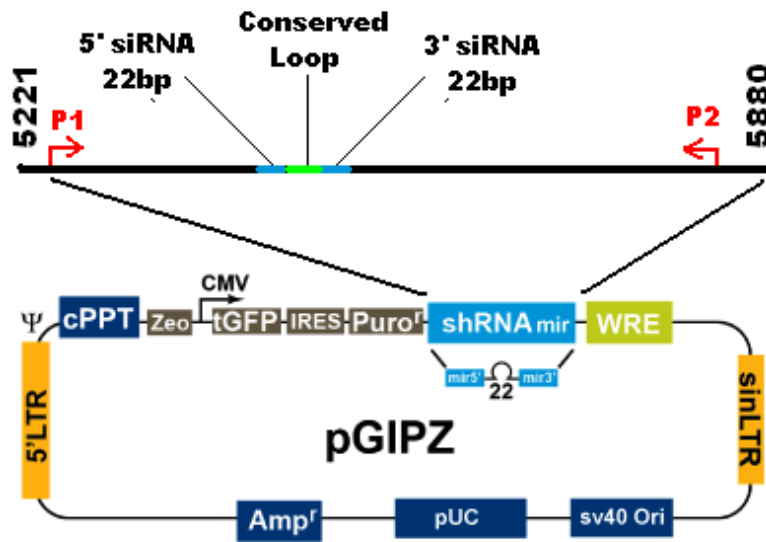
#### *Isolation of Genomic DNA*

Genomic DNA was isolated from the WS1 colonies that resulted from the shRNA screen. These colonies were isolated by spot trypsinization, and cultured in 24-well plates

separate from each other. When cells reached ~80% confluence on the 24-well plate, they were trypsinized, and genomic DNA was isolated using Quiagen's Gentra® Puregene® Core Kit A.

### *Polymerase Chain Reaction*

Genomic DNA extracted from each screen was amplified via Polymerase Chain Reaction (PCR) using primers that allowed amplification of a 602 bp region of the pGIPZ plasmid construct shown below in Figure-6. Amplification was facilitated by Taq DNA Polymerase purchased from New England Biolabs. The 602 bp region amplified included the siRNA construct sequence (shown as blue in the diagram) and the conserved loop sequence (shown as green in the diagram) that was expressed in the cells of a given colony. The amplified DNA from each colony was sent for sequence verification.



**Primer 1: X76 Forward** **Primer 2: M100 Reverse**  
**5'-acgtcgaggtycccgaagga-3'** **5' aagcagcgtatccacatagcgt -3'**

**Conserved Loop**  
**5'-atgtgaagcccacagatgta-3'**

\*Figure Adapted from Open Biosystems, Expression Arrest GIPZ lentiviral shRNAmir library product information.

**Figure 6: PCR Amplification of shRNA-miR Insert.** Primers were designed to amplify a 602 bp region of the shRNA-miR insert. This 602 bp region included the 22 bp 5' siRNA and 3' siRNA which form a loop in the mRNA by base pairing, leading to RNA interference.

### Sequencing

DNA amplified via PCR was purified and sent to Genewiz Inc. for sequencing.

### Clone Confirmation

Two of the clones, AHCYL1 and CDC42BPA, identified in the shRNA gene knockdown screen were ordered individually from Open Biosystems for further study. These specific shRNA constructs came in plasmid form, and were transformed, isolated, and packaged into lentivirus as described above. WS1 cells were infected with either non-silencing control shRNA, shRNA that knocked down AHCYL1, or shRNA that knocked

down CDC42BPA. This initial infection was carried out at MOI 0.5 in separate 100cm dishes, alongside mock infected controls.

When mock control plates were clear, each of the three samples were plated on 6-well plates (4 wells each) at  $3.5 \times 10^6$  for  $\beta$ -gal and crystal violet staining, and on four 100cm plates at  $5 \times 10^5$ ; three of these plates were used for subsequent infection with Smurf2, Smurf2 C716A, or GFP, the fourth plate was used for RNA extraction.

After mock infected plates were clear, each sample was plated at  $3.5 \times 10^6$  cells per well on 6-well plates (4 wells for each sample) for  $\beta$ -gal and crystal violet staining, and at  $2 \times 10^4$  cells per well on 6-well plates (6 wells per sample).

#### *RNA Isolation*

RNA was isolated from cells pre-Smurf2 exposure to analyze the level of gene knockdown in the presence of each shRNA construct. RNA was isolated using a Qiagen RNeasy® Mini Kit.

#### *RT-PCR*

Invitrogen Superscript® II Reverse Transcriptase was used to facilitate cDNA synthesis via RT-PCR.

#### *Crystal Violet Staining*

Crystal Violet staining was performed in 6-well plates that were plated at  $3.5 \times 10^4$  cells per well 72 hours after plating. Cells were washed with PBS, then stained with 1% Crystal Violet in 3% ethanol for 5 minutes. Cells were washed again, then photographed at 10X magnification.

### *Growth Curves*

Growth curves were created from 6-well plates that were plated at  $5 \times 10^4$  cells per well for each sample. One well of each sample was counted each day for six days (starting the day after the cells were plated) in a Beckman Coulter® Z1 Particle Counter three times. The average of the three counts was recorded for each sample.

## RESULTS

The purpose of this project was to identify potential genes in the senescence pathway that lie downstream of Smurf2 in order to facilitate a better understanding of senescence.

### Production and Testing of shRNA Viral Library

Transfections were performed in HEK-293T cells to package all virus types (shRNA-expressing and Smurf2-expressing) used in this project. DsRed was included in all transfections alongside packaging constructs as a marker for transfection efficiency. Figure-7 below shows a representative DsRed fluorescence in HEK-293T pre-transfection and post-transfection. The strong dsRed fluorescence in the right panel indicates an efficient transfection of the plasmid construct into the HEK-293T cells.

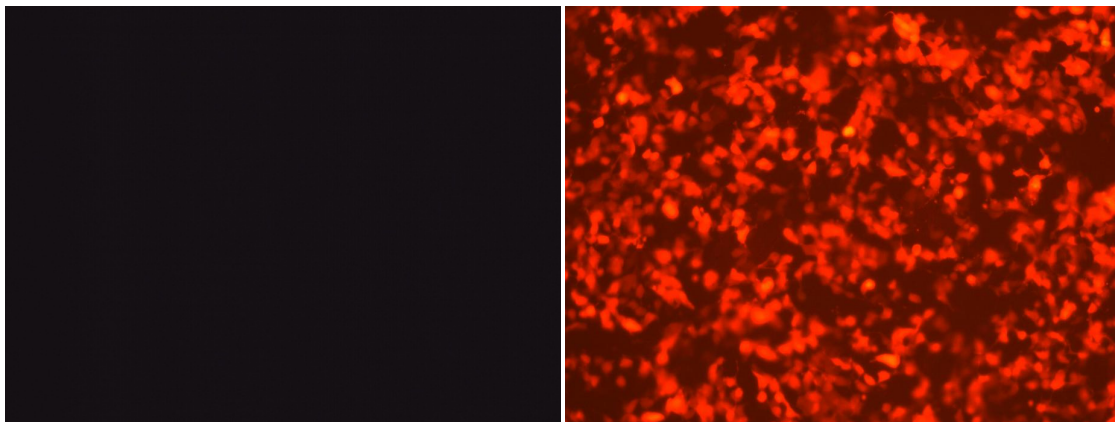


**Figure 7: HEK-293T Transfection Efficiency.** HEK-293T transfection efficiency is shown by dsRed fluorescence pre-transfection (left) and post-transfection (right) for a typical transfection carried out in this project.



The Colony Forming Units, or CFU, for each of the viruses packaged in this project were determined in HT1080 cells. This was accomplished by plating HT1080 cells in p60 plates at  $5 \times 10^4$  cells per plate, then infecting with virus. Viral infection was performed for all the pools of the library, all Smurf2 transfections, CDC42BPA transfections, and AHCYL1 transfections. All viral supernatants were plated at 10ul, 1ul, and 0.1ul per plate, and were run alongside a control with polybrene only. Figure-8 below shows example crystal violet stained plates from shRNA pool #1 fifteen days post infection. In this case, plate B shows a countable number of colonies, and was used to determine the viral titer.

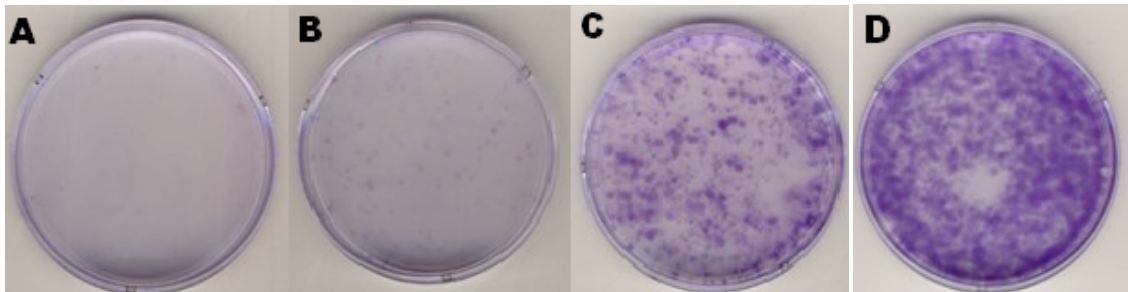


**Figure 8: shRNA pool #1 HT1080 CFU Plates.** A. Mock Infection. B. 0.1ul shRNA pool #1 supernatant added, 97 colonies on plate indicating a CFU of 970virus/mL. C. 1.0ul shRNA pool#1 viral supernatant added, too many colonies to count. D. 10.0ul shRNA pool#1 supernatant.

### shRNA Screen for Genes Involved in Smurf2-Induced Senescence

Genomic DNA extracted from the screens run in this project contained a single integrated shRNA construct, which was amplified using the two primers shown in Figure-6. These primers amplified a 602bp region of the shRNA construct that included the 22bp siRNA regions. The amplified DNA was run on a gel to assess the purity of each sample before sending samples for sequencing. Figure-9 below shows a gel separation of some of the constructs amplified in this MQP.

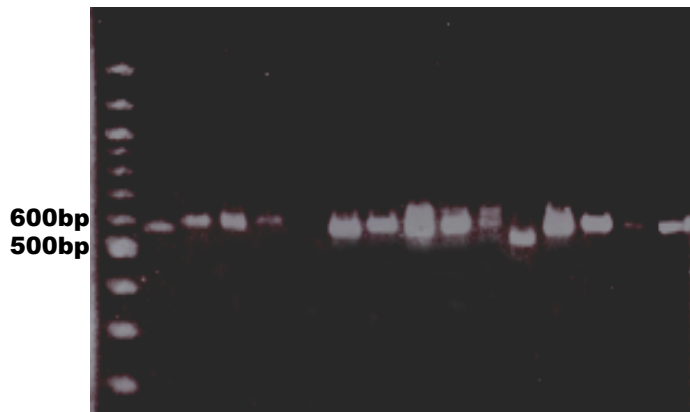


**Figure 9: PCR Purity Gel.** 3ul of each PCR amplified sample was run on a gel alongside a 100bp ladder to assess the purity of each sample. Samples in lanes 2-5, 7-8, 10, and 13-14 from this gel were deemed pure enough to sequence.

Table I below shows the genes identified in the screens run in this MQP. The first screen challenged the cells with Smurf2 wild-type expression, the second with Smurf2 C716A expression. Thirteen genes were identified in total from 24 colonies that escaped senescence in the two screens. Genes were identified from the sense siRNA sequence using BLAST and BLAT software. Table I shows the genes that were targeted, the amount of base pairs that match between the gene and the siRNA, the sense siRNA sequence, and the chromosome locus of the gene identified. S-adenosylhomocysteine hydrolase-like 1 and CDC42-binding protein kinase alpha isoform A are highlighted in this table because they were studied further in this MQP in an attempt to confirm that they operate downstream of Smurf2 in senescence.

Pool #	Smurf2 Type	Gene name	Identity Match	Chromosome Locus	Sense siRNA sequence 5' -> 3'
1	Normal	Inter-genic sequence	22/22	20q13.12	CCCAGCCTTAGTATTGATTCTA
2	Ligase Mutant	Hypothetical protein LOC9729 (C6orf174)	21/22	6q22.33	ACAACAGAGTCTGCATTGCAAA
2	Normal	V2LHS_214049	21/22	12q12	CGCTAATGATGCTGCAACATAA
2	Normal	N/A	No match	None	AGCTCCTCTGTTAATGAGATTA
<b>3</b>	<b>Ligase Mutant</b>	<b>S-adenosylhomocysteine hydrolase-like 1</b>	<b>21/22</b>	<b>1p13.3</b>	<b>ACCCATTTCTTAGCTGCTGAAA</b>
3	Normal	Zinc finger, RAN-binding domain containing 1	21/22	10q26.13	CGGAACTTGAAGTAGACTTTAA
3	Normal	Ubiquitin domain-containing protein 2	21/22	5q35.1	CAGGACTATGTTGTACAGGTTA
4	Ligase Mutant	Abhydrolase domain containing 7	21/22	1p22.1	ACCATTCATCGACAGAATTATA
5	Ligase Mutant	Arylsulfatase D isoform	21/22	Xp22.3	CGCATGGCTTATATGGTGATAA
<b>6</b>	<b>Ligase Mutant</b>	<b>CDC42-binding protein kinase alpha isoform A</b>	<b>21/22</b>	<b>1q42.11</b>	<b>CGCATCTAATATCATAACAGAA</b>
6	Ligase Mutant	Zinc finger protein, X-linked	22/22	Xp22.11	CGCAAATGGATGACAATGAAAT
6	Normal	Kelch-like 10	21/22	17q21.2	CGCTGAGTACTTCATGAACAAT
6	Normal	N/A	No Match	None	CCGGCTGAATTATCGGTGATAA

**Table I: Thirteen Candidate Genes That May Act Downstream of Smurf2.** Table I is a compilation of all sequencing data collected in this project. The genes that each siRNA targeted are shown, along with the amount of nucleotides that match between the siRNA and the gene. Further research supported the hypothesis that S-adenosylhomocysteine hydrolase-like 1 (AHCYL1) and CDC42-binding protein kinase alpha isoform A (CDC42BPA) might act downstream of Smurf2 in senescence. Some Clones were isolated from a ligase mutant Smurf2 challenge screen and some were isolated from a wild-type Smurf2 challenge screen.

### Verification of AHCYL1 and CDC42BPA

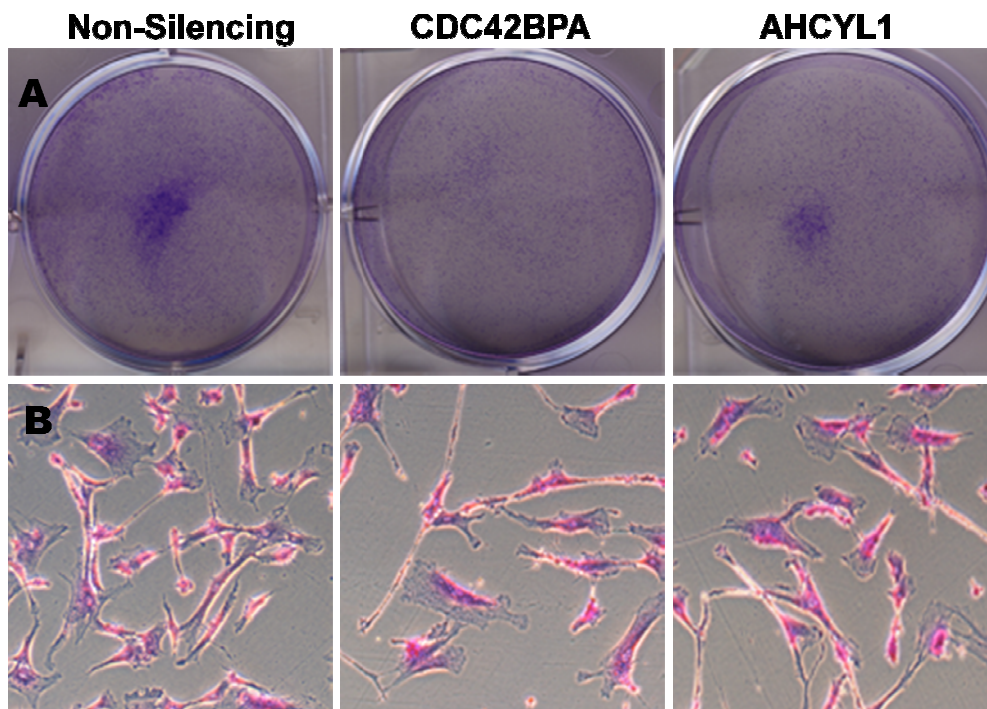
S-adenosylhomocysteine hydrolase-like 1 (AHCYL1) was one of the genes from Table-1 that I attempted to confirm as acting downstream of Smurf2 in senescence in this

MQP. Figure-10 below shows AHCYL1's protein sequence aligned with its homolog protein AHCYL2's sequence. Deficiency of AHCYL2 has been shown to allow fibroblasts to escape p53-induced senescence (Berns et al., 2004). The two proteins are strongly conserved, so AHCYL1 may also play a role in senescence escape.

		1		50
Human AHCYL1	(1)	-----		
Human AHCYL2	(1)	MSVQVVSAAAAAKVPEVELKDLSPSEAESQLGLSTAAVGAMAPPAGGGDP		
Consensus	(1)			
		51		100
Human AHCYL1	(1)	---MSMPDAMPPLPGVG-----EELKQAKEI		
Human AHCYL2	(51)	EAPAPAAERPVPVPGSGPAAALSPAAGKVPQASAMKRSDPHHQQRHRD		
Consensus	(51)	D PLPG G Q		
		101		150
Human AHCYL1	(23)	EDAKEYSFMATVTKAP---KKQIQFADDMQEFTKFPTKTGRRSLSRISISQ		
Human AHCYL2	(101)	GGEALVSPDGTVTEAPRTVKKQIQFADQKQEFNKRPTKI GRRSLSRISISQ		
Consensus	(101)	S ATVT AP KKQIQFAD QEF K PTK GRRSLSRISISQ		
		151		200
Human AHCYL1	(70)	SSTDSYSSAASYTDSDDDEVSPREKQQTNSKGSSNFCVKNIKQAEFGRRE		
Human AHCYL2	(151)	SSTDSYSSAASYTDSDDDETSPRDKQQKNSKGSSDFCVKNIKQAEFGRRE		
Consensus	(151)	SSTDSYSSAASYTDSDDDE SPRDKQQ NSKGSS FCVKNIKQAEFGRRE		
		201		250
Human AHCYL1	(120)	IEIAEQDMSALISLRKRAQGEKPLAGAKIVGCTHITAQTAVLIETLALG		
Human AHCYL2	(201)	IEIAEQEMPALMALRRAQGEKPLAGAKIVGCTHITAQTAVLMETLALG		
Consensus	(201)	IEIAEQDM ALIALRRAQGEKPLAGAKIVGCTHITAQTAVLIETL ALG		
		251		300
Human AHCYL1	(170)	AQCRWSACNIYSTQNEVAAALAEAGVAVFAWKGESEDDFWWCIDRCVNMD		
Human AHCYL2	(251)	AQCRWAACNIYSTLNEVAAALAEAGFPVFAWKGESEDDFWWCIDRCVNVE		
Consensus	(251)	AQCRWAACNIYST NEVAAALAEAG VFAWKGESEDDFWWCIDRCVNMD		
		301		350
human AHCYL1	(220)	GWQANMILDDGGDLTHWVYKKYPNVFKKIRGIVEESVTGVHRLYQLSKAG		
human AHCYL2	(301)	GWQPNMILDDGGDLTHWIYKKYPNMFKKIKGIVEESVTGVHRLYQLSKAG		
Consensus	(301)	GWQ NMILDDGGDLTHWIYKKYPNMFKKIKGIVEESVTGVHRLYQLSKAG		
		351		400
human AHCYL1	(270)	KLCVPAMNVNDSVTKQKFDNLCCRESILDGLKRTTDMFVGGKQVVCVCGY		
human AHCYL2	(351)	KLCVPAMNVNDSVTKQKFDNLCCRESILDGLKRTTDMFVGGKQVVCVCGY		
Consensus	(351)	KLCVPAMNVNDSVTKQKFDNLCCRESILDGLKRTTDMFVGGKQVVCVCGY		
		401		450
human AHCYL1	(320)	GEVKGCCAALKALGAIVYITEIDPICALQACMDGFRVVKLNEVIRQVDV		
human AHCYL2	(401)	GEVKGCCAALKAMGSIVYVTEIDPICALQACMDGFRVVKLNEVIRQVDI		
Consensus	(401)	GEVKGCCAALKALGAIVYITEIDPICALQACMDGFRVVKLNEVIRQVDI		
		451		500
human AHCYL1	(370)	VITCTGNKNVVTREHLDRMKNSCIVCNMGHSNTEIDVTLRTPELTWERV		
human AHCYL2	(451)	VITCTGNKNVVTREHLDRMKNSCIVCNMGHSNTEIDVASLRTPELTWERV		
Consensus	(451)	VITCTGNKNVVTREHLDRMKNSCIVCNMGHSNTEIDV SLRTPELTWERV		
		501		550
human AHCYL1	(420)	RSQVDHVIWPDGKRVVLLAEGRLLNLSCTVPTFVLSITATTQALALIEL		
human AHCYL2	(501)	RSQVDHVIWPDGKRIVVLLAEGRLLNLSCTVPTFVLSITATTQALALIEL		
Consensus	(501)	RSQVDHVIWPDGKRIVVLLAEGRLLNLSCTVPTFVLSITATTQALALIEL		
		551		600
human AHCYL1	(470)	YNAPEGRYKQDVYLLPKKMDEYVASLHLPSTFAHLTELTDQAKYLGLNK		
human AHCYL2	(551)	YNAPEGRYKQDVYLLPKKMDEYVASLHLPTFAHLTELTDQAKYLGLNK		
Consensus	(551)	YNAPEGRYKQDVYLLPKKMDEYVASLHLPSTFAHLTELTDQAKYLGLNK		
		601		611
human AHCYL1	(520)	NGPFKPNYYRY		
human AHCYL2	(601)	NGPFKPNYYRY		
Consensus	(601)	NGPFKPNYYRY		

**Figure 10: AHCYL1 and AHCYL2 Protein Alignment.** The alignment above shows very high homology between AHCYL1 and AHCYL2. The alignment was created using Invitrogen's Vector NTI software. The comparison between the proteins in the final 500 C-terminal amino acids showed 90.2% homology and 4.4% similarity.

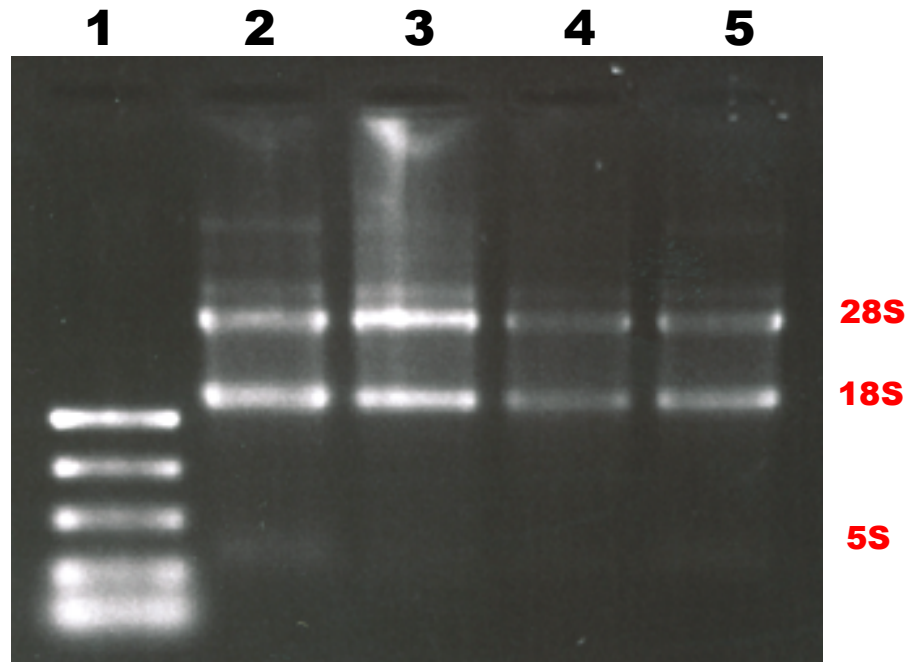
Figure-11 below shows control (pre-Smurf2 expressing viral infection) crystal violet staining of the cells of the confirmation screen; which was run in this project in attempt to confirm whether AHCYL1 and CDC42BPA allow escape of Smurf2 induced senescence. Figure-11 shows the cells 11 days post infection, with shRNA constructs encoding siRNA that corresponded to AHCYL1 and CDC42BPA knockdown (see Table I for construct sequences). This figure suggests that knockdown of AHCYL1 does not affect cell density compared to non-silencing shRNA, and that knockdown of CDC42BPA corresponds to a decrease in cell density compared to non-silencing control prior to GFP/Smurf2 C716A challenge.



**Figure 11: Crystal Violet Staining of Infected WS1 Cells.** WS1 cells 11 days post infection with Non-silencing shRNA, CDC42BPA silencing shRNA, or AHCYL1 silencing shRNA are shown. Cells were stained with crystal violet (A). Magnification at 10X shows cell morphology of crystal violet stained cells (B).

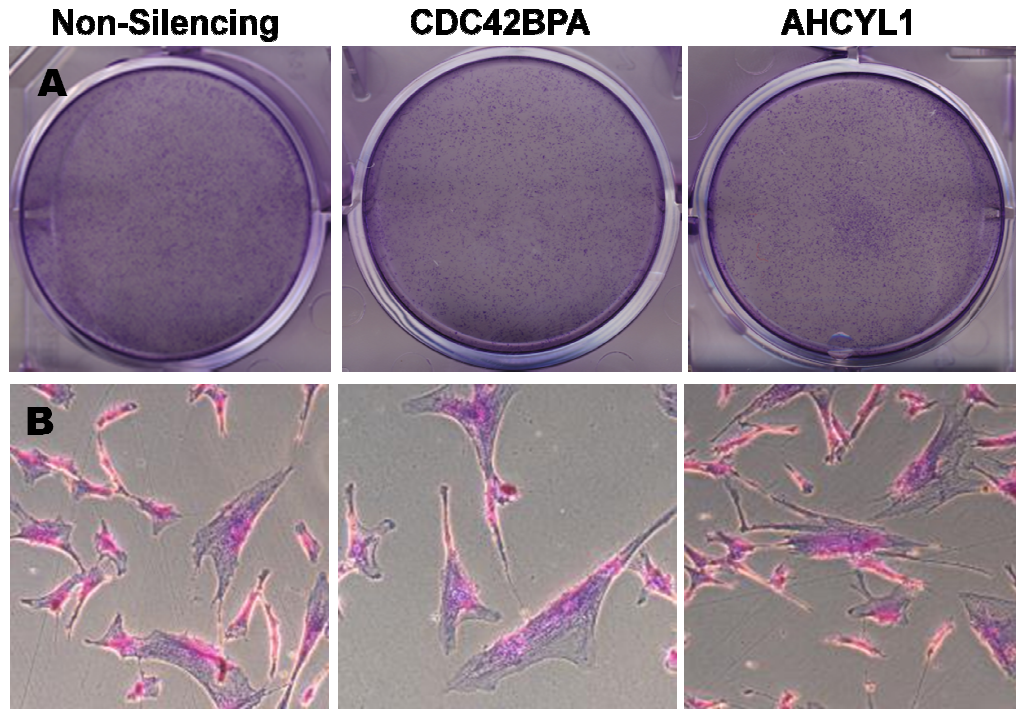
Figure-12 below shows the purity and integrity of the RNA samples extracted from WS1 cells infected with non-silencing shRNA, AHCYL1 shRNA, or CDC42BPA

shRNA. The 28S, 18S, and 5S ribosomal RNA subunits are labeled. The clarity of these bands indicates that RNase activity has not substantially degraded the RNA extracted from these cells; and that RNA isolated is pure enough for analysis with RT-qPCR.



**Figure 12: RNA Purity and Integrity.** Figure 12 shows the purity of the RNA samples extracted from WS1 cells (lane 2), WS1 cells transfected with a non-silencing shRNA (lane 3), WS1 cells transfected with CDC42BPA (lane 4), and WS1 cells transfected with AHCYL1 (lane 5). Lane 1 contained a PCR marker. The 28s, 18s, and 5s ribosomal RNA subunits are labeled.

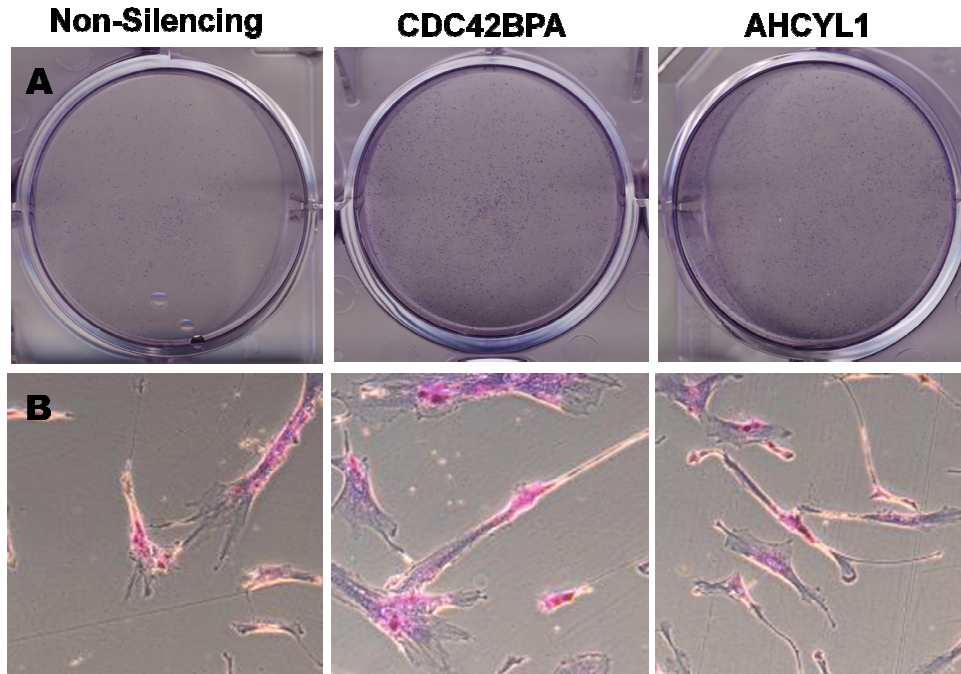
Figure-13 below shows crystal violet staining of the cells of the confirmation screen 10 days after infection with GFP. This secondary infection acts as a control for the Smurf2 C716A challenge. This data correlates with that of Figure-11; cells with non-silencing and AHCYL1 knockdown have similar density, and cells with CDC42BPA knockdown have lower density.



**Figure 13: GFP Control Secondary Infection of WS1 Cells.** WS1 cells were infected with GFP expressing virus after infection with either; non-silencing shRNA, CDC42BPA shRNA, or AHCYL1 shRNA. Row 1 shows crystal violet plates, row 2 shows of crystal violet stained cells at 10X magnification.

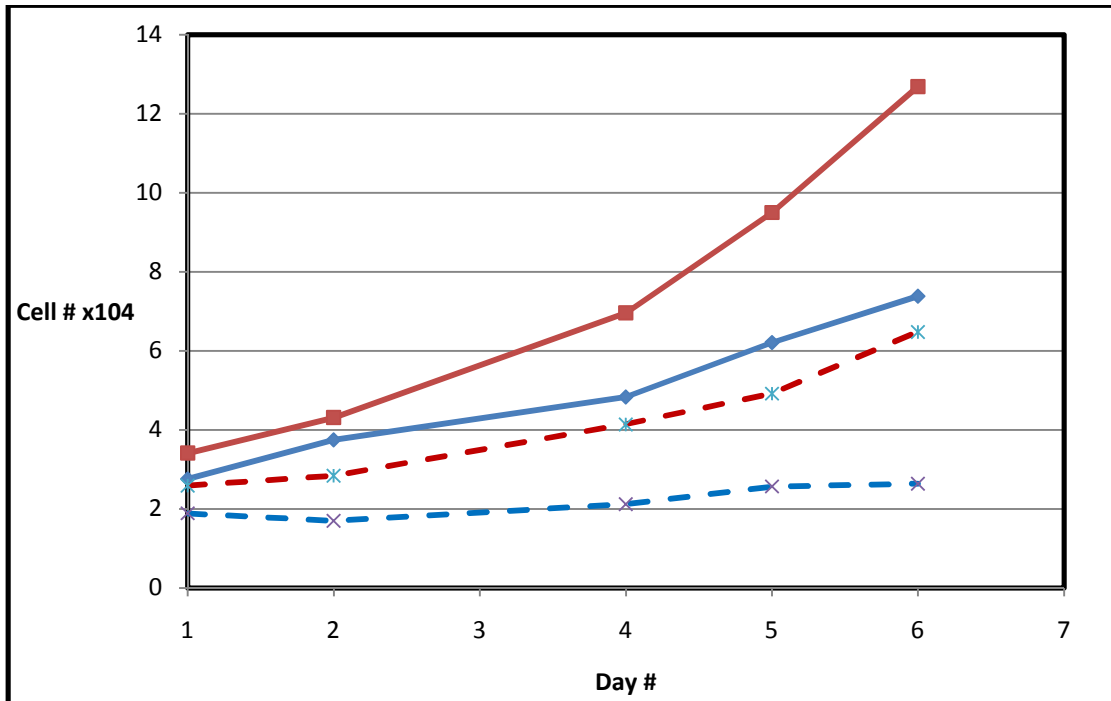
Figure-14 below shows crystal violet staining of the cells of the confirmation screen 10 days after infection with Smurf2 C716A. Crystal violet staining shows lower density in the non-silencing shRNA compared to CDC42BPA and AHCYL1 knockdown.





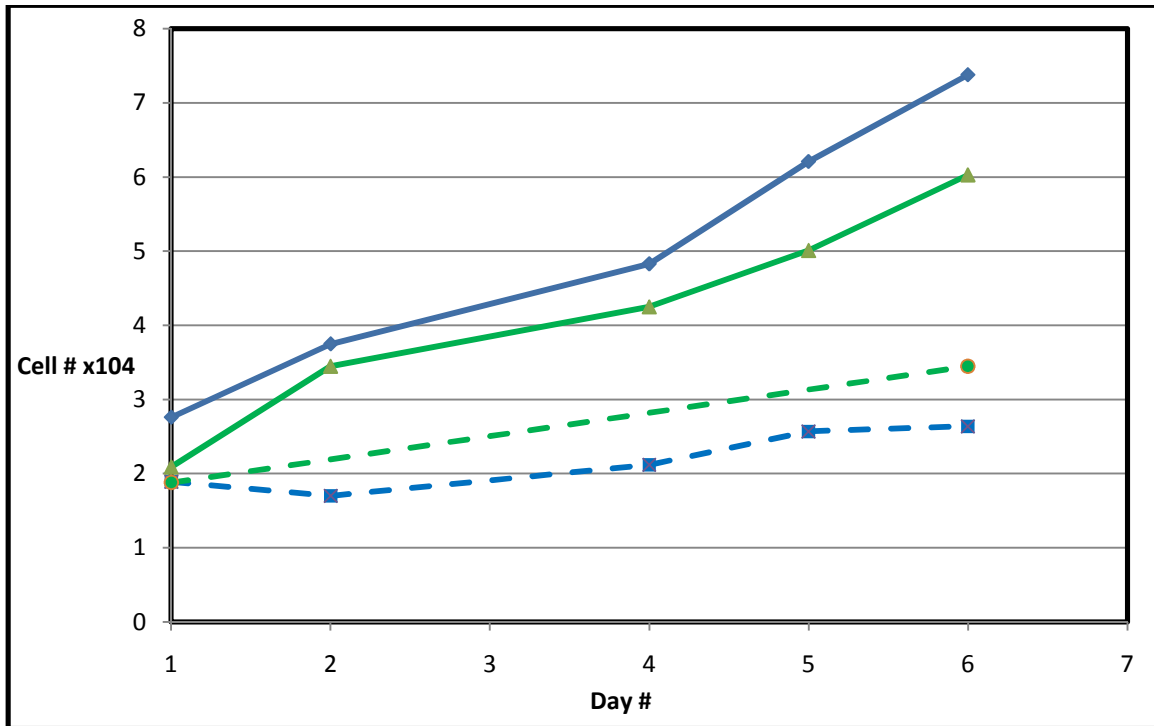
**Figure 14: Smurf2 C716A Challenge Secondary Infection of WS1 Cells.** WS1 cells were infected with Smurf2 C716A expressing virus after infection with either; non-silencing shRNA, CDC42BPA shRNA, or AHCYL1 shRNA. Row 1 shows crystal violet plates, row 2 shows close up view of crystal violet stained cells at 10X magnification.

Figure-15 below shows growth curve data collected from the AHCYL1 and non-silencing knockdown cells in the confirmation screen that were infected with either GFP (control) or Smurf2 C716A (challenge). These cells were plated four days post infection with GFP or C716A (day 1 count corresponds to five days post infection). The data show that AHCYL1/GFP growth rate is faster than non-silencing/GFP. The data also showed that Smurf2 C716A challenge in AHCYL1 knockdown (dashed red line) correlates with a significant escape of senescence versus non-silencing knockdown (dashed blue line).



**Figure 15: AHCYL1 Knockdown Correlates with Escape of Smurf2 C716A Induced Senescence.** Cell count data was collected for WS1 cells transfected with non-silencing shRNA/GFP (solid blue), non-silencing shRNA/Smurf2 C716A (dashed blue), AHCYL1 shRNA/GFP (solid red), and AHCYL1 shRNA/Smurf2 C716A (dashed red). Data shows that AHCYL1 cells challenged with Smurf2 C716A partially escape the control senescence phenotype (shown by non-silencing shRNA/Smurf2 C716A).

Figure-16 below shows growth curve data collected from the CDC42BPA and non-silencing knockdown cells in the confirmation screen that were infected with either GFP (control) or Smurf2 C716A (challenge). These cells were plated four days post infection with GFP or C716A (day 1 count corresponds to five days post infection). The data show that CDC42BPA/GFP growth rate is comparable to that of non-silencing/GFP. The data also showed that Smurf2 C716A challenge in CDC42BPA knockdown (dashed green line) does not correlate with a significant escape of senescence versus non-silencing knockdown (dashed blue line).



**Figure 16: CDC42BPA Knockdown Does Not Correlate with Significant Escape of Smurf2 Induced C716A Senescence.** Cell count data was collected for WS1 cells transfected with non-silencing shRNA/GFP (solid blue), non-silencing shRNA/Smurf2 C716A (dashed blue), CDC42BPA shRNA/GFP (solid green), and CDC42BPA/Smurf2 C716A (dashed green). Note that cell number was only sufficient to plate two wells for CDC42BPA/C716A cells; which were counted on days 1 and 6. This data does not show a significant escape from the C716A induced senescence.

## DISCUSSION

This project was successful in using shRNA gene knockdown screening to identify candidate genes downstream of Smurf2 in senescence. Thirteen such genes were identified from the two screens run in this project. Two of the genes identified (AHCYL1 and CDC42BPA) were investigated further in an attempt to confirm the correlation between the knockdown of these genes and escape of Smurf2-induced senescence. The preliminary data collected indicates that knockdown of AHCYL1 allows partial escape of senescence, while knockdown of CDC42BPA does not allow any significant escape from senescence.

### **AHCYL1 and CDC42BPA**

AHCYL1 and CDC42BPA were two genes of interest identified in this project as potentially allowing escape from Smurf2-induced senescence in WS1 fibroblasts. The individual shRNA constructs that were pulled out of our screen were reordered and assessed individually in WS1 fibroblasts for escape of Smurf2 senescence. The information below briefly describes these two genes and provides the reasoning for studying them further.

#### *AHCYL1*

S-adenosylhomocysteine hydrolase-like 1, or AHCYL1 (a.k.a. IRBIT), was a gene that my screen suggested, when knocked down, allowed WS1 fibroblasts to escape Smurf2-induced senescence. AHCYL1 is a protein that catalyses the reaction S-adenosyl-L-homocysteine + H<sub>2</sub>O = adenosine + L-homocysteine. The identification of this gene

was intriguing since AHCYL2, a homolog protein of AHCYL1, has been implicated as a gene which plays a role in senescence (Berns et al., 2004). AHCYL2 has been shown to allow fibroblasts to escape senescence when knocked-down via RNAi. This escape of senescence in response to AHCYL2 knockdown was shown to act through the p53 senescence pathway and not through the pRB pathway (Berns et al., 2004). Knockdown of AHCYL2 did not affect p53 levels, but did lead to decreased p21 mRNA and protein levels, suggesting that AHCYL2 might act downstream of p53 (Berns et al., 2004). This downstream effect in senescence of p53 on AHCYL2, coupled with Smurf2's link to p53 induced senescence suggests that Smurf2 could affect AHCYL2.

Could AHCYL1 function as its homolog does in senescence? In order to hypothesize the answer to this, AHCYL1 and AHCYL2 were aligned using Invitrogen's Vector NTI software. This alignment showed very high similarity (Figure-10). The similarity was greatest in the final 500 C-terminal amino acids of AHCYL1/AHCYL2, which showed 90.2% homology plus 4.4% similarity. The high level of homology between AHCYL1 and AHCYL2 brought forth the hypothesis that AHCYL1 might be downstream of Smurf2-p53 in fibroblast senescence (see Figure-17).

### *CDC42BPA*

CDC42 binding protein kinase alpha, or CDC42BPA (a.k.a MRCK or MRCK $\alpha$ ), was another gene that our screen suggested, when knocked down, allowed WS1 fibroblasts to escape Smurf2-induced senescence. CDC42BPA acts alongside CDC42 in the MRCK-CDC42 nuclear movement signaling pathway (Ghomes et al., 2005). CDC42 is a Rho GTPase that has also been identified as an effector of multiple signal transduction pathways, and has been shown to influence transcription factor activity

(Etienne-Manneville and Hall, 2002). Proteins in the Rho signaling pathway have been shown to contribute to cell cycle regulation, specifically in the progression of T-cells from G1 to S phase (Cantrell, 1998), and the initiation of S1 in quiescent fibroblasts (Olsen et al., 1995). This point is of particular interest because replicative senescence has been shown to stop fibroblasts from leaving G0/G1 and initiating S-phase. This information coupled with the discovery that CDC42BPA is regulated by Notch1 levels, which are regulated by p53, allowed us to hypothesize that CDC42BPA may act downstream of p53 (Lefort et al., 2007) (see Figure-17).

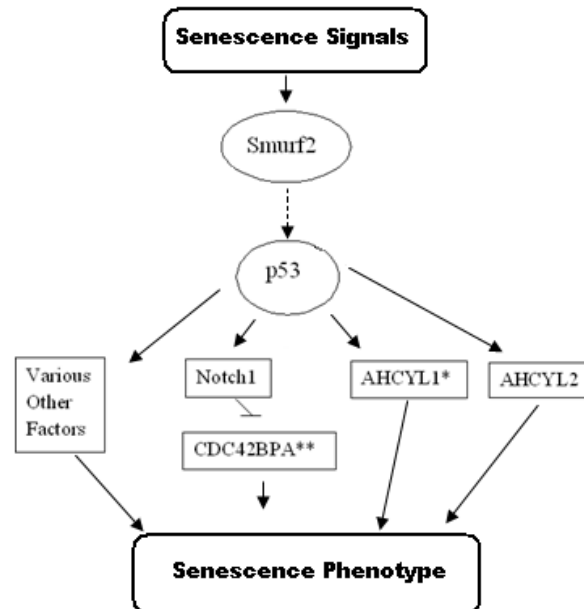


**Figure 17: AHCYL1's and CDC42BPA's Hypothesized Role in Senescence.** CDC42BPA has been shown to act downstream of p53 via a Notch1 intermediate. AHCYL2, a close relative of AHCYL1, has been shown to act downstream of p53 allowing us to hypothesize AHCYL1 might act downstream of p53. p53 has been shown to change the transcriptional levels of many other genes, some of which this figure presumes influence the senescence signal.

## Future Directions

The shRNA constructs shown in Table I of this project were found in only a single colony in the screen; suggesting that the screen was not run to saturation. If the

screen were saturated, one would expect to pick up multiple colonies containing the same shRNA construct. In order to ensure saturation of the screen, the same shRNA pools should be screened in the same manner until some of the shRNA constructs are isolated from Smurf2-induced senescence escaping cells multiple times.

In order to identify as many genes downstream of Smurf2 as possible, another set of screens should be run using the 35,000 other unique shRNA constructs that are part of the human pGIPZ library (65,000 constructs total). This would ensure that all genes effected by the pGIPZ shRNA library are tested for escape from Smurf2-induced senescence.

All of the constructs in Table I should be ordered and screened in the same way AHCYL1 and CDC42BPA were in this project in order to identify which candidates allow significant escape from senescence. Furthermore, any gene whose expression arrest correlates with Smurf2-induced senescence escape should be studied further to understand its precise role in the senescence pathway.

RNA extracted in this project from WS1 cells (uninfected, non-silencing, AHCYL1, and CDC42BPA) should be analyzed for changes in transcript levels of key genes in the senescence pathway. First, this analysis should determine the amount of knockdown that occurs in the target genes in response to shRNA infection. Also, transcript levels for Smurf2, p53, and p21 should be analyzed to see if the knockdown of AHCYL1 or CDC42BPA correlates with changes in expression of these genes.

## BIBLIOGRAPHY

Atadja, P, Wong H, Garkavtsev I, Veillette C, and Riabowol K. 1995. Increased activity of p53 in senescing fibroblasts. *Proc Natl Acad Sci USA* 92: 8348-52.

Berns K, Hijmans EM, Mullenders J, Brummelkamp TR, Velds A, Heimerikx M, Kerkhoven RM, Madiredjo M, Nijkamp W, Weigelt B, Agami R, Ge W, Cavet G, Linsley PS, Beijersbergen RL, Bernards R. 2004. A large-scale RNAi screen in human cells identifies new components of the p53 pathway. *Nature* 428: 431-437.

Blackburn EH. 2001. Switching and signaling at the telomere. *Cell* 106:661–673.

Bodnar AG, Ouellette M, Frolkis M, Holt SE, Chiu CP, Morin GB, Harley CB, Shay JW, Lichtsteiner S, Wright WE. 1998. Extension of life-span by introduction of telomerase into normal human cells. *Science* 279: 349–352.

Brown JP, Wei W, Sedivy JM. 1997. Bypass of senescence after disruption of p21CIP1/WAF1 gene in normal diploid human fibroblasts. *Science* 277:831-834.

Campisi J, Goberdhan P, Dimri GP, Nehlin JO, Testori A, Yoshimoto K. 1996. Coming of age in culture. *Exp Gerontology*. 31: 7-12.

Cantrell D. 1998. Lymphocyte signalling: a coordinating role for Vav? *Curr. Biol.* 8:535-538.

Chen PL, Chen Y, Bookstein R, Lee WH. 1990. Genetic mechanisms of tumor suppression by the human p53 gene. *Science* 250: 1576-1580.

Chen HI, Sudol, M. 1995. The WW domain of Yes-associated protein binds a proline-rich ligand that differs from the consensus established for Src homology 3-binding modules. *PNAS* 92: 7819-7823.

Dimri GP, Lee X, Basile G, Acosta M, Scott G, Roskelley C, Medrano EE, Linskens M, Rubelj I, Pereira-Smith O, et al. 1995. A biomarker that identifies senescent human cells in culture and in aging skin in vivo. *Proc Natl Acad Sci USA* 92: 9363–9367.

Etienne-Manneville S, Hall A. 2002. Rho GTPases in cell biology. *Nature* 420:629-635.

Ezhevsky SA, Nagahara H, Vocero-Akbani AM, Guis DR, Wei MC, Dowdy SF. 1997. Hypo-phosphorylation of the retinoblastoma protein (pRb) by cyclin D:Cdk4/6 complexes results in active pRb. *PNAS* 94: 10699-10704.

Gomes ER, Jani A, Gundersen GG. 2005. Nuclear Movement Regulated by Cdc42, MRCK, Myosin, and Actin Flow Establishes MTOC Polarization in Migrating Cells. *Cell* 121:451-463.



- Goberdhan DP. 2005. What has senescence got to do with cancer? *Cancer Cell* 6: 505-512.
- Goldstein S. 1990. Replicative senescence: The human fibroblast comes of age. *Science* 249: 1129–1133.
- Hara E, Smith R, Parry D, Tahara H, Stone S, Peters G. 1996. Regulation of p16CDKN2 expression and its implications for cell immortalization and senescence. *Mol Cell Biol* 16:859-867.
- Harley CB. 1991. Telomere loss: mitotic clock or genetic time bomb? *Mutat Res* 256:271-282.
- Hayflick L, Moorhead PS. 1961. The serial cultivation of human diploid cell strains. *Exp Cell Res* 25: 585–621.
- Herbig U, Jobling WA, Chen BPC, Chen DJ, Sedivy JM. 2004. Telomere Shortening Triggers Senescence of Human Cells through a Pathway Involving ATM, p53, and p21CIP1, but Not p16INK4a. *Molecular Cell* 14: 501–513.
- Itahana K, Zou Y, Itahana Y, Martinez JL, Beausejour C, Jacobs JL, Lohuizen M, Band V, Campisi J, Goberdhan DP. 2003. Control of the Replicative Life Span of Human Fibroblasts by p16 and the Polycomb Protein Bmi-1. *Mol and Cell Biology*. 23: 389–401.
- Kim NW, Piatyszek MA, Prowse KR, Harley CB, West MD, Ho PLC, Coviello GM, Wright WE, Weinrich SL, Shay JW. 1994. Specific association of human telomerase activity with immortal cells and cancer. *Science* 266: 2011-2016.
- Lefort K, Mandinova A, Ostano P, Kolev V, Calpini V, Kolfshoten I, Devgan V, Lieb J, Raffoul W, Hohl D, Neel V, Garlick J, Chiorino G, Dotto GP. 2007. Notch1 is a p53 target gene involved in human keratinocyte tumor suppression through negative regulation of ROCK1/2 and MRCK $\alpha$  kinases. *Genes & Dev*. 21: 562-577.
- Lin X, Liang M, Feng XH. 2000. Smurf2 Is a Ubiquitin E3 Ligase Mediating Proteasome-dependent Degradation of Smad2 in Transforming Growth Factor- $\beta$  Signaling. *J. Biol. Chem.*, 47: 36818-36822.
- Olson MF, Ashworth A, Hall A. 1995. An essential role for Rho, Rac and CDC42 GTPases in cell cycle progression through G1. *Science* 269:1270-1272.
- Pereira-Smith OM, Smith, JR. 1988. Genetic analysis of indefinite division in human cells: identification of four complementation groups. *Proc Natl Acad Sci USA* 85: 6042-6046.
- Sherwood SW, Rush D, Ellsworth JL, Schimke RT. 1988. Defining cellular senescence in IMR-90 cells: A flow cytometric analysis. *Proc Natl Acad Sci USA* 85: 9086–9090.

Shippen-lentz D, Blackburn EH. 1989. Telomere Terminal Transferase Activity from *Euplotes crassus* Adds Large Numbers of TTTTGGGG Repeats onto Telomeric Primers *Mol and Cell Bio.* 9: 2761-2764.

Stein GH, Drullinger LF, Soulard A, Dulic V. 1999. Differential roles for cyclin-dependent kinase inhibitors p21 and p16 in the mechanisms of senescence and differentiation in human fibroblasts. *Mol. Cell. Biol.* 19: 2109–2117.

Watson JD. 1972. Origin of concatemeric T7 DNA. *Nat New Biol.* 239:197-201.

Wei W, Herbig U, Wei S, Dutriaux A, Sedivy JM. 2003. Loss of retinoblastoma but not p16 function allows bypass of replicative senescence in human fibroblasts. *EMBO reports* 4: 1061-1065.

Zhang X, Mar V, Zhou W, Harrington L, Robinson MO. 1999. Telomere shortening and apoptosis in telomerase-inhibited human tumor cells. *Genes Dev* 13: 2388–2399.

Zhang H, Cohen SN. 2004. Smurf2 up-regulation activates telomere-dependent senescence. *Genes Dev* 18: 3028-3040.

Zhang H. 2007. Molecular Signaling and Genetic Pathways of Senescence: Its Role in Tumorigenesis and Aging. *JCP* 210: 567-574.